Curved boundary corrections to nodal line statistics in chaotic billiards

2005 J. Phys. A: Math. Gen. 38 1491

(http://iopscience.iop.org/0305-4470/38/7/006)

INSTITUTE OF PHYSICS PUBLISHING JOURNAL OF PHYSICS A: MATHEMATICAL AND GENERAL

J. Phys. A: Math. Gen. **38** (2005) 1491–1504 doi:10.1088/0305-4470/38/7/006

Curved boundary corrections to nodal line statistics in chaotic billiards

C T Wheeler

School of Mathematics, University of Bristol, University Walk, Bristol BS8 1TW, UK

Received 12 October 2004, in final form 2 December 2004
Published 2 February 2005
Online at stacks.iop.org/JPhysA/38/1491

Abstract
A Gaussian random wavefunction that satisfies Dirichlet and Neumann conditions locally on a convex circular boundary is introduced. The average of the square of the wavefunction and its derivatives are computed and their asymptotics studied in the semi-classical limit. The mean nodal line length $\langle L \rangle$ is calculated and the first order boundary effect shown to be of order $\log k$, where k is the wavenumber. In the limit of vanishing boundary curvature (large boundary radius) these results are shown to approach those for a straight wall boundary.

PACS numbers: 03.65.Sq, 05.45.Mt

1. Introduction

We study the distribution of the zeros of quantum wavefunctions in two-dimensional classically chaotic billiard systems. For systems with time reversal symmetry, and therefore real wavefunctions, these zeros form lines, called nodal lines, which split the domain up into regions (nodal domains) where the wavefunction is either positive or negative. In systems with no time reversal symmetry the wavefunctions are complex and the zeros are nodal points, where the nodal lines of the real part of the wavefunction cross those of the imaginary part.

The Gaussian random wave model, put forward by Berry in his seminal 1977 paper [1], uses an ensemble of plane waves with random directions and phases to model the wavefunctions of classically chaotic quantum systems. This model accurately predicts the bulk statistical properties of these wavefunctions but in the original form is unable to describe the effect of boundaries upon these statistics. The range of applications could be increased dramatically if these boundary effects are incorporated into the model.

The statistical properties of nodal lines have been the subject of considerable recent interest (e.g. [2–6]). The local nodal line density in and around the classically forbidden region was explored by Bies and Heller [7]. The effect of a straight boundary on the density and other statistics of nodal lines was first investigated by Berry [8] (henceforth simply referred to as Berry). The standard Gaussian random wavefunction was split into terms which were odd and even about the line $Y = 0$, taking the appropriate component to satisfy the boundary condition. This approach was extended to mixed boundary conditions by Berry and Ishio [9]. Bies *et al* [10] calculated the boundary adapted wavefunction and two-point correlation function for wedge-shaped geometries with the interior angle an integer divisor of π and also the semi-infinite rectangular corridor. Urbina and Richter [11] wrote the two-point correlation function for a general billiard in terms of the Green function averaged over a small energy window and by assuming that the statistics of the system are Gaussian showed that all statistics can be derived from this function. In [12], they combine the methods of the previous paper with approximations to the Green function in the semi-classical limit from which an approximate two-point correlation function can be derived. The leading order contribution (in the wavenumber k) is shown to come from the direct paths with the next order deriving from paths that hit the boundary once; this order of approximation is sufficient to produce the large wavenumber asymptotics of the previously published results [8–10].

Our purpose here is to look at the effect of a convex curved boundary on the density of nodal lines and average nodal line length. We consider a circular scatterer in an infinite domain and conjecture that the results derived from this geometry may be extended to more general cases. We take the wavefunction to be Berry's random wave model far away from the scatterer and adapt the wavefunction to satisfy our boundary conditions (either Dirichlet or Neumann) on the scatterer. The standard plane-wave definition [1] is decomposed into spherical waves written in terms of Bessel functions of the first kind (denoted by $J_n(x)$). The boundary condition is satisfied by using a superposition of this standard model and a randomized ensemble of spherical waves using Hankel functions of the first kind. We will focus on real wavefunctions. The extension to complex wavefunctions should be obvious at each stage. Explicit expressions can then be calculated for statistics of the wavefunction. Taking an approximation and then computing the large wavenumber asymptotics of the derivatives of the square of the wavefunction up to second order allows us to calculate the nodal line density and mean nodal line length. As in Berry's paper we find that there is a long-range boundary effect in both statistics that is independent of our choice of Neumann or Dirichlet boundary conditions. Our results are consistent with those of Urbina and Richter [13] and complement theirs in that we derive our results by finding an exact representation for the wavefunction and then using the semi-classical asymptotics to find our results rather than starting from a semi-classical approximation.

This paper is structured as follows. In section 2 we discuss our wavefunction, calculate the average of the wavefunction and its first order derivatives squared and their asymptotics. The quantity we then study is the average of the total length of nodal lines for a wavefunction $u(r)$ given by,

$$L = \int\int_{A_B} \delta(u(r))|\nabla u(r)|\, \mathrm{d}^2 r. \tag{1.1}$$

Taking the average over random wavefunctions requires us to calculate probability distributions for u_α and u_r (where r and α are polar coordinates). This is done in section 3 using a method which mirrors that of Berry and will utilize the averages from the previous section. A necessary step in this calculation is finding an expression for the density of nodal lines. We then examine how these statistics evolve with distance from the boundary.

2. Boundary adapted Gaussian random wavefunction

The standard Gaussian random function that was introduced by Berry [1] and is used to model the eigenfunctions of chaotic quantum billiards in the semi-classical limit can be written in

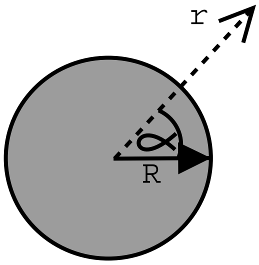

Figure 1. Our geometry—we use polar coordinates r and α. The boundary has radius R.

the form,

$$u(r,\alpha) = \sqrt{\frac{2}{J}} \sum_{j=1}^{J} \mathrm{e}^{\,\mathrm{i}kr\cos(\alpha+\theta_j)+\mathrm{i}\phi_j} \tag{2.1}$$

in polar coordinates. Here the θ_j and ϕ_j are independent random variables uniformly distributed in the range $[0, 2\pi)$. Provided $J \gg 1$ in this expression we know from the central limit theorem that the statistics of the wavefunction will have a Gaussian distribution. We model the wavefunction in an infinite domain with a circular scatterer of radius R centred at the origin using polar coordinates as seen in figure 1. We assume either Dirichlet or Neumann boundary conditions on the scatterer. Using the well-known expansion of a plane wave as a sum of spherical waves we have that

$$u(r,\alpha) = \sqrt{\frac{2}{J}} \sum_{j=1}^{J} \sum_{n=-\infty}^{\infty} \mathrm{i}^n J_n(kr)\, \mathrm{e}^{\,\mathrm{i}(n(\alpha+\theta_j)+\phi_j)}. \tag{2.2}$$

We use the Hankel function of the first kind (denoted here by $H_n(x)$) as a solution of the Bessel equation that is linearly independent of $J_n(x)$ to satisfy the boundary condition. This gives a wavefunction adapted locally to match a Dirichlet boundary condition ($u = 0$) on $r = R$:

$$u_{\mathrm{Dirichlet}}(r,\alpha) = \sqrt{\frac{2}{J}} \sum_{j=1}^{J} \sum_{n=-\infty}^{\infty} \mathrm{i}^n \left(J_n(kr) - \frac{J_n(kR)}{H_n(kR)} H_n(kr) \right) \mathrm{e}^{\,\mathrm{i}(n(\alpha+\theta_j)+\phi_j)}. \tag{2.3}$$

For Neumann conditions ($u_r = 0$) on $r = R$ the corresponding expression is

$$u_{\mathrm{Neumann}}(r,\alpha) = \sqrt{\frac{2}{J}} \sum_{j=1}^{J} \sum_{n=-\infty}^{\infty} \mathrm{i}^n \left(J_n(kr) - \frac{J_n'(kR)}{H_n'(kR)} H_n(kr) \right) \mathrm{e}^{\,\mathrm{i}(n(\alpha+\theta_j)+\phi_j)}. \tag{2.4}$$

These wavefunctions have the required property that as $r \to \infty$ the boundary term vanishes and therefore they look like the isotropic Gaussian random wave model (2.2) at a large distance away from the boundary.

The real part of the Dirichlet wavefunction is

$$\begin{aligned} u(r,\alpha) = \sqrt{\frac{2}{J}} \sum_{j=1}^{J} \sum_{n=-\infty}^{\infty} J_n(kr) \cos\left(n\left(\alpha+\theta_j+\frac{\pi}{2}\right)+\phi_j\right) - \frac{J_n(kR)}{J_n(kR)^2+Y_n(kR)^2} \\ \times \left[(J_n(kr)J_n(kR)+Y_n(kr)Y_n(kR)) \cos\left(n\left(\alpha+\theta_j+\frac{\pi}{2}\right)+\phi_j\right) \right. \\ \left. - (J_n(kr)Y_n(kR)-J_n(kR)Y_n(kr)) \sin\left(n\left(\alpha+\theta_j+\frac{\pi}{2}\right)+\phi_j\right) \right]. \end{aligned} \tag{2.5}$$

$Y_n(x)$ is the Bessel function of the second kind. We need to calculate certain averages of these wavefunctions in order to compute the density function, this is done by integrating over ϕ_j and θ_j and is denoted by $\langle \ldots \rangle$. We use the results

$$\begin{aligned}\frac{1}{4\pi^2}\int_0^{2\pi}\int_0^{2\pi} &\sin\left(n\left(\alpha+\theta_i+\frac{\pi}{2}\right)+\phi_i\right)\sin\left(m\left(\alpha+\theta_j+\frac{\pi}{2}\right)+\phi_j\right)\mathrm{d}\phi_j\,\mathrm{d}\phi_i \\ &= \frac{1}{4\pi^2}\int_0^{2\pi}\int_0^{2\pi}\cos\left(n\left(\alpha+\theta_i+\frac{\pi}{2}\right)+\phi_i\right)\cos\left(m\left(\alpha+\theta_j+\frac{\pi}{2}\right)+\phi_j\right)\mathrm{d}\phi_j\,\mathrm{d}\phi_i \\ &= \frac{1}{2}\delta_{ij}\delta_{nm}\end{aligned} \tag{2.6}$$

and

$$\int_0^{2\pi}\int_0^{2\pi}\cos\left(n\left(\alpha+\theta_i+\frac{\pi}{2}\right)+\phi_i\right)\sin\left(m\left(\alpha+\theta_j+\frac{\pi}{2}\right)+\phi_j\right)\mathrm{d}\phi_j\,\mathrm{d}\phi_i = 0, \tag{2.7}$$

where δ_{ij} is the Kronecker delta symbol. The relevant non-zero averages are given by,

$$\begin{aligned}\langle u^2\rangle = 1 - \sum_{n=-\infty}^{\infty}\frac{J_n(kR)}{J_n(kR)^2+Y_n(kR)^2}&[J_n(kR)(J_n(kr)^2-Y_n(kr)^2) \\ &+2J_n(kr)Y_n(kr)Y_n(kR)] = B\end{aligned} \tag{2.8}$$

$$\begin{aligned}\langle u_r^2\rangle = \frac{k^2}{2}\Bigg(1-2\sum_{n=-\infty}^{\infty}&\frac{J_n(kR)}{J_n(kR)^2+Y_n(kR)^2} \\ &\times[J_n(kR)(J_n'(kr)^2-Y_n'(kr)^2)+2J_n'(kr)Y_n'(kr)Y_n(kR)]\Bigg) = D_r\end{aligned} \tag{2.9}$$

$$\begin{aligned}\langle u_\alpha^2\rangle = \sum_{n=-\infty}^{\infty} n^2\Bigg(J_n(kr)^2 + &\frac{J_n(kR)}{J_n(kR)^2+Y_n(kR)^2} \\ &\times[J_n(kR)(J_n(kr)^2-Y_n(kr)^2)+2J_n(kr)Y_n(kr)Y_n(kR)]\Bigg) = D_\alpha\end{aligned} \tag{2.10}$$

$$\begin{aligned}\langle uu_r\rangle = -\sum_{n=-\infty}^{\infty}\frac{kJ_n(kR)}{J_n(kR)^2+Y_n(kR)^2}&[J_n(kR)(J_n(kr)J_n'(kr)-Y_n(kr)Y_n'(kr)) \\ &+Y_n(kR)(J_n(kr)Y_n'(kr)+Y_n(kr)J_n'(kr))] = K_r.\end{aligned} \tag{2.11}$$

The labelling matches that of Berry. The corresponding results for the Neumann conditions are easily obtained from these results by replacing $J_n(kR)$ and $Y_n(kR)$ with their respective derivatives.

2.1. Deriving the asymptotics

We now wish to look at the asymptotics of these formulae as $k \to \infty$. We can use the large order n asymptotics [14, equation 9.3.1] for our summands to show that they tend to zero very quickly as $n \to \infty$. In fact for $|n| > \frac{\exp kR}{2}$ these terms become very small and can be neglected. Therefore we look at only finitely many terms. In order to simplify the expression we use the large argument (and fixed order) Bessel function asymptotics for the denominator so as $k \to \infty$ [14, equation 9.2.28]

$$J_n(kR)^2+Y_n(kR)^2 = \frac{2}{\pi kR}+\frac{4n^2-1}{4\pi(kR)^3}+O\left(\frac{n^4}{k^5}\right). \tag{2.12}$$

The corresponding expression for the Neumann terms is [14, equation 9.2.30]

$$J_n'(kR)^2 + Y_n'(kR)^2 = \frac{2}{\pi kR} - \frac{4n^2 - 3}{4\pi(kR)^3} + O\left(\frac{n^4}{k^5}\right). \tag{2.13}$$

We use the first order term in these asymptotics. This has the advantage of making our denominator independent of n. Checking the numerator using the large n asymptotics as above we find that our sum is still convergent. The exception to this is the third term in the $\langle u_\alpha^2 \rangle$ expression, equation (2.10). This will be considered in section 2.2. The error caused by making this approximation is of lower order than the asymptotics we use it to calculate. We proceed by expressing the Bessel functions in their integral forms [14, equation 9.1.22].

$$J_n(z) = \frac{1}{\pi}\int_0^\pi \cos(z\sin\theta - n\theta)\,\mathrm{d}\theta \tag{2.14}$$

$$Y_n(z) = \frac{1}{\pi}\int_0^\pi \sin(z\sin\theta - n\theta)\,\mathrm{d}\theta - \frac{1}{\pi}\int_0^\infty (\mathrm{e}^{nt} + \mathrm{e}^{-nt}\cos(n\pi))\,\mathrm{e}^{-z\sinh t}\,\mathrm{d}t. \tag{2.15}$$

We ignore the second integral term in equation (2.15) because it is of higher order in z. Using the double angle formulae we convert the integrand from a product of trigonometric functions into a sum of trigonometric functions each of which may be integrated separately. Exchanging the order of integration and summation enables us to use the formula

$$\sum_{n=-\infty}^{\infty} \mathrm{e}^{\mathrm{i}nt} = 2\pi \sum_{n=-\infty}^{\infty} \delta(2n\pi - t), \tag{2.16}$$

which may be proved using the Poisson summation formula. This allows us to consider at most a couple of terms in the sum because our integration variables are limited to the range $[0, \pi]$. The delta function also means that the integration over one of the variables is trivial. We are left with the triple integral of a trigonometric function with nonlinear argument. We are interested in the large k asymptotics and therefore we can use the method of stationary phase. This entire process is covered in appendix A. As $k \to \infty$ the asymptotics are:

$$\langle u^2 \rangle \sim 1 \mp \sqrt{\frac{R}{\pi kr(r-R)}}\cos\left(2k(r-R) - \frac{\pi}{4}\right) \tag{2.17}$$

$$\langle u_r^2 \rangle \sim \frac{k^2}{2}\left(1 \pm 2\sqrt{\frac{R}{\pi kr(r-R)}}\cos\left(2k(r-R) - \frac{\pi}{4}\right)\right) \tag{2.18}$$

$$\langle uu_r \rangle \sim \pm k\sqrt{\frac{R}{\pi kr(r-R)}}\sin\left(2k(r-R) - \frac{\pi}{4}\right). \tag{2.19}$$

In all the formulae we consider henceforth the upper/lower signs correspond to the results for Dirichlet/Neumann conditions respectively. The expressions are obviously not defined when $r = R$, this is a legacy of our asymptotic approximation. The agreement between these asymptotics and the exact expressions is very good, even for small values of k, although the divergence as $r \to R$ is marked (see figure 2). Also shown in figure 2 are numerical results for these statistics found by averaging the square of the wavefunction and its derivatives over five thousand realizations, these also show a good agreement with our results.

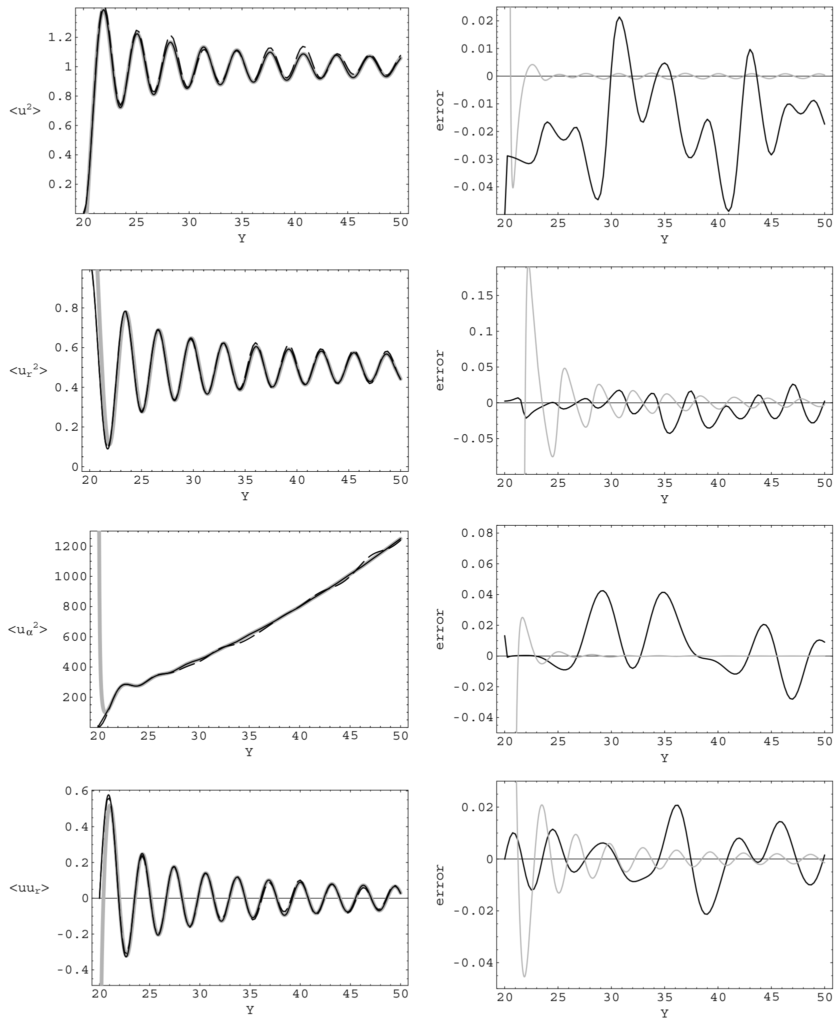

Figure 2. Averages of the Dirichlet wavefunction. The left-hand plot in each case shows the exact formula (black line) against the asymptotic formula (thick grey line). Also shown (dashed line) in these plots are the numerical results found by averaging these statistics across 5000 realizations. For these plots we took, $k = 1$, $R = 20$. The right-hand plots are of the relative error between the exact formulae, the asymptotics (grey line) and the numerics (black line). For the $\langle uu_r \rangle$ error plot we show just the unscaled error because the function oscillates around zero.

2.2. *Computing* $\langle u_\alpha^2 \rangle$

It is not possible to use the method outlined in the previous section on the expression

$$\sum_{n=-\infty}^{\infty} \frac{n^2 J_n(kr) J_n(kR) Y_n(kr) Y_n(kR)}{J_n(kR)^2 + Y_n(kR)^2}. \tag{2.20}$$

This is because if we replace the denominator with its asymptotics to first order we get a divergent sum. We can avoid doing this by differentiating equation (2.8) twice with respect to α,

$$\langle uu_{\alpha\alpha} \rangle = -\langle u_\alpha^2 \rangle. \tag{2.21}$$

We now refer back to our original Schrödinger equation in polar coordinates and multiply both sides by our wavefunction u and take averages,

$$u_{rr} + \frac{1}{r}u_r + \frac{1}{r^2}u_{\alpha\alpha} = -k^2 u \tag{2.22}$$

$$\langle uu_{rr}\rangle + \frac{1}{r}\langle uu_r\rangle + \frac{1}{r^2}\langle uu_{\alpha\alpha}\rangle = -k^2\langle u^2\rangle. \tag{2.23}$$

If we now differentiate equation (2.8) twice again but with respect to r this time, calling the right-hand side $B(r)$ to fit in with our earlier notation we get,

$$\langle uu_{rr}\rangle = \tfrac{1}{2}B''(r) - \left\langle u_r^2\right\rangle. \tag{2.24}$$

Combining equations (2.21), (2.23) and (2.24) we can now find an expression for $\left\langle u_\alpha^2\right\rangle$ consisting only of quantities that we have already found asymptotics for,

$$\left\langle u_\alpha^2\right\rangle = r^2\left(k^2\langle u^2\rangle + \frac{1}{r}\langle uu_r\rangle + \frac{1}{2}B''(r) - \left\langle u_r^2\right\rangle\right). \tag{2.25}$$

This allows us to work out the leading order contribution; this corresponds to

$$\left\langle u_\alpha^2\right\rangle \sim \sum_{n=-\infty}^{\infty} n^2 J_n(kr)^2 = \frac{k^2r^2}{2}. \tag{2.26}$$

The terms of order $k^{\frac{3}{2}}$ that come from the $k^2\langle u^2\rangle$ and $\left\langle u_r^2\right\rangle$ asymptotics cancel, so to recover the next order contribution we need to look at higher order asymptotics for these expressions. This is described in detail in appendix B. The final expression is

$$\left\langle u_\alpha^2\right\rangle \sim \frac{k^2r^2}{2}\left(1 \mp \pi\left(\frac{R}{\pi kr(r-R)}\right)^{\frac{3}{2}}\sin\left(2k(r-R) - \frac{\pi}{4}\right)\right). \tag{2.27}$$

We can use the results from this section to calculate probability distributions (denoted by convention by P) for u using the fact that u and its linear functionals are Gaussian distributed, the results we use in section 3 are:

$$P(u_\alpha) = \sqrt{\frac{1}{2\pi D_\alpha}}\exp\left(\frac{-u_\alpha^2}{2D_\alpha}\right) \tag{2.28}$$

$$P(u=0, u_r) = \frac{1}{2\pi\sqrt{BD_r - K_r^2}}\exp\left(\frac{-Bu_r^2}{2\left(BD_r - K_r^2\right)}\right). \tag{2.29}$$

The fact that these distributions turn out to be Gaussian is consistent with, and may be seen as a justification of, one of the assumptions made by Urbina and Richter [12].

3. Mean nodal line length

By taking the average of equation (1.1) we find that [8]

$$\langle L\rangle = \frac{k}{2\sqrt{2}}\int\int_{A_B}\rho_L(r)\,\mathrm{d}^2r, \tag{3.1}$$

where the mean nodal line density, $\rho_L(r)$, is defined by

$$\rho_L(r) = 2\sqrt{2}\langle\delta(u)|\nabla_R u|\rangle. \tag{3.2}$$

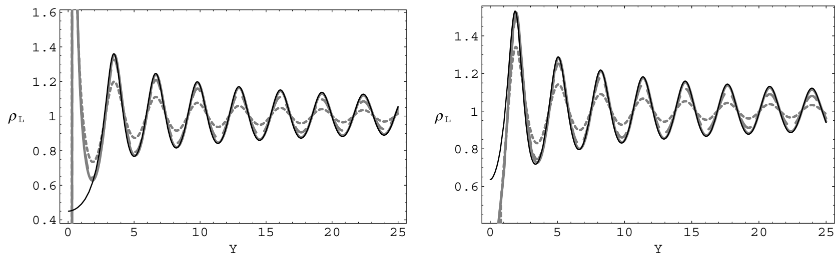

Figure 3. Mean nodal line density ρ_L for Dirichlet and Neumann boundary conditions respectively. The thin black line is the exact formula for the flat boundary as given in [9]. The thick grey lines are calculated using the asymptotics of the averages and equation (3.6). Going from dashed to full, the lines correspond to having a scatterer of radius $R = 2$, 20 and 200.

The prefactor of $2\sqrt{2}$ in this expression ensures that $\rho_L(r) \to 1$ as $r \to \infty$ and will cancel with the reciprocal prefactor in equation (3.1). Using the formulae from the previous section we find that,

$$\rho_L(r) = 2\sqrt{2}\int_{-\infty}^{\infty}\int_{-\infty}^{\infty} P(u=0,u_r)P(u_\alpha)\sqrt{u_r^2 + \frac{u_\alpha^2}{r^2}}\,\mathrm{d}u_r\,\mathrm{d}u_\alpha \tag{3.3}$$

$$= \frac{1}{\pi\sqrt{\pi D_\alpha\left(BD_r - K_r^2\right)}} \times \int_{-\infty}^{\infty}\int_{-\infty}^{\infty} \exp\left(\frac{-B}{2}\left(\frac{u_r^2}{BD_r - K_r^2} + \frac{u_\alpha^2}{BD_\alpha}\right)\right)\sqrt{u_r^2 + \frac{u_\alpha^2}{r^2}}\,\mathrm{d}u_r\,\mathrm{d}u_\alpha \tag{3.4}$$

$$= \frac{2\sqrt{2}D_\alpha\left(BD_r - K_r^2\right)}{\pi r^2}\int_0^{\frac{\pi}{2}}\left(\frac{BD_\alpha}{r^2}\cos^2\psi + \left(BD_r - K_r^2\right)\sin^2\psi\right)^{-\frac{3}{2}}\mathrm{d}\psi \tag{3.5}$$

$$= \frac{2\sqrt{2\left(BD_r - K_r^2\right)}}{\pi B}\mathbf{E}\left(1 - \frac{BD_\alpha}{r^2\left(BD_r - K_r^2\right)}\right), \tag{3.6}$$

where $\mathbf{E}$ denotes the elliptic integral of the first kind. This expression can be used for both Dirichlet and Neumann conditions. Plots of both cases are shown in figure 3. It is obvious that for both types of boundary condition we get a repulsion of nodal lines by the boundary although this effect is much stronger for the Dirichlet conditions. The repulsion is a consequence of any nodal lines intersecting the boundary doing so perpendicularly for both types of boundary condition.

Looking at $\rho_L(r)$ far away from the boundary we can see that it oscillates about 1 with decaying amplitude. Using equation (3.5) and the asymptotics for the averages, equations (2.17)–(2.19), we can use a binomial expansion to give asymptotics as $k \to \infty$

$$\rho_L(r) = 1 \pm \sqrt{\frac{R}{\pi kr(r-R)}}\cos\left(2k(r-R) - \frac{\pi}{4}\right) - \frac{R}{32\pi kr(r-R)} + O\left(\frac{R}{kr(r-R)}\right). \tag{3.7}$$

The term that interests us is the leading order non-oscillatory term so we will not consider the oscillatory term at that order $(1/k)$ or any higher order terms. Clearly this expression is dependent upon the radius of the scatterer R; alternatively we can think of this in terms of the curvature of the boundary $1/R$. It is clear that as the radius of the scatterer decreases the effect of the boundary on the nodal structure decreases with it. This is because the increased curvature of the boundary means that any point in the domain is further away from an average point on the boundary and therefore experiences its effect to a lesser degree. This phenomenon is visible in figure 3.

If we consider this argument in the reciprocal limit and look at what happens as the curvature gets small, that is $R \to \infty$, we approach the case where locally the circumference of the circle approximates a straight line. In this regime, if we take Y to be the scaled distance from the boundary and the distance from the boundary to be small compared to the radius of the scatterer,

$$Y = k(r - R) \qquad \frac{R}{r} \simeq 1 \tag{3.8}$$

we find that equation (3.7) for ρ_L exactly matches the density of nodal lines that Berry [8] found for the straight line boundary. In this regime we can relate the derivatives of polar coordinates with those of Berry's scaled Cartesian coordinate system by

$$\frac{\partial}{\partial Y} = \frac{1}{k}\frac{\partial}{\partial r} \qquad \frac{\partial}{\partial X} = \frac{1}{kr}\frac{\partial}{\partial \alpha}. \tag{3.9}$$

If we now compare the asymptotics of our averages with the large argument asymptotics of Berry's results we find that the match is exact. Therefore we can reproduce Berry's results for $\rho_L(Y)$ and consequently $\langle L\rangle$ in this limit.

These statistics can also be obtained using the technique of Urbina and Richter [13]. In this method the multiple reflection expansion of the Green function for the system is made. The two-point correlation function is approximated by averaging a further semiclassical approximation to the multiple reflection Green function terms over a small energy window. The approximate two-point correlation function is then used to calculate nodal line density. With careful manipulation of the energy window the result follows from the first two terms of the multiple reflection expansion, the terms coming from the direct path and the classical one-bounce trajectories respectively.

We can separate the bulk and boundary terms in the density by writing,

$$\rho_L(\tau) = 1 + (\rho_L(\tau) - 1). \tag{3.10}$$

The leading order non-oscillatory boundary term reflects an infinite deficit in mean nodal line length when a torus of infinite radius extending from the boundary is considered. We examine the average behaviour of this quantity by integrating the boundary terms over part of an annulus. We take the domain to be between $\theta = 0$ and $1/kR$ in the angular direction, this ensures that the inner boundary is always one wavelength wide, independent of the boundary radius. In the radial direction we average over a scaled domain between $\tau = kr$ and the boundary at $\tau = kR$.

$$\begin{aligned}\int_0^{\frac{1}{kR}}\int_{kR}^{kr}(\rho_L(\tau) - 1)\tau\,\mathrm{d}\tau\,\mathrm{d}\theta &= -\frac{1}{32\pi}\ln(k(r-R)) + C\\ &\quad \pm\frac{1}{2}\sqrt{\frac{r}{\pi kR(r-R)}}\sin\left(2k(r-R) - \frac{\pi}{4}\right) + O\left(\sqrt{\frac{r}{kR(r-R)}}\right),\end{aligned} \tag{3.11}$$

where C is some constant term which is not determined. In the limit as $R \to \infty$ both the domain and the formula match Berry's strip result [8, equation 16]. As in that case the leading order boundary contribution to this quantity is independent of whether we are considering Neumann or Dirichlet boundary conditions.

To examine this effect on the billiard we integrate the density over the entire domain. The main problem in this case is in deciding the upper limit for the radial integration, if we assume that the billiard is roughly toroidal in shape then we can express the upper limit in terms of the area of the billiard,

$$r = \sqrt{\frac{A_B}{\pi} + R^2}. \tag{3.12}$$

Integrating in the angular direction gives a factor of 2π to each term. By interference the oscillatory terms vanish and therefore the leading order boundary term is the logarithmic divergence from the $(r(r-R))^{-1}$ term in the ρ_L expression.

$$\langle L\rangle = \frac{kA_B}{2\sqrt{2}} - \frac{C_S}{64\pi\sqrt{2}} \ln(k(\sqrt{A_B + A_S} - \sqrt{A_S})) + O(k^0), \tag{3.13}$$

where A_S and C_S denote the area and the circumference of the scatterer respectively. The constant here is not determined and would depend upon the upper limit of the r integration, we expect a contribution from the outer boundary as well. As in Berry's case the leading order correction depends upon the logarithm of the area of the billiard, however in our case the total boundary correction is smaller than Berry's.

It is important to check whether statistical fluctuations due to variations in the nodal line length between states are of higher order than our boundary corrections because in this case our results would not be visible in experimental data. This was done by Berry [8] for the standard isotropic Gaussian random wavemodel. The large k asymptotics of this result are

$$(\delta L)^2 \approx \frac{A_B}{256\pi} \ln(k\sqrt{A_B}). \tag{3.14}$$

Fortunately, as in the straight line case we find that this fluctuation is just smaller than our boundary correction.

4. Discussion

The main result of this work is that the average nodal line length has the same leading order logarithmic boundary term for a convex circular boundary that Berry calculated for the straight-line boundary. Again we find that this logarithmic term is independent of the type of boundary condition that we have chosen. It is clear from our results that the magnitude of these effects is dependent upon the curvature of this boundary, and that as the curvature decreases the results approach those for the straight boundary.

Acknowledgments

The author would like to thank his supervisors Jon Keating and Jens Marklof for their help and guidance in this work and Ian Williams for many helpful conversations. This work was completed whilst sponsored by the EPSRC.

Appendix A. Asymptotics of the averages

To provide an example of our method for calculating asymptotics of our averages we describe this process in detail for the $\langle u^2\rangle$ expression. We start by expressing the Bessel functions in terms of their integral identities; however, we ignore the second term in the $Y_n(x)$ integral expansion (equation (2.15)) because it is of lower order than our dominant terms.

$$\sum_{n=-\infty}^{\infty} J_n(kR)^2(J_n(kr)^2 - Y_n(kr)^2)$$
$$\simeq \sum_{n=-\infty}^{\infty} \frac{1}{\pi^4}\int_0^\pi\int_0^\pi\int_0^\pi\int_0^\pi \mathrm{d}\theta\,\mathrm{d}\phi\,\mathrm{d}\alpha\,\mathrm{d}\beta\cos(kR\sin\theta - n\theta)\cos(kR\sin\phi - n\phi)$$
$$\times(\cos(kr\sin\alpha - n\alpha)\cos(kr\sin\beta - n\beta)$$
$$-\ \sin(kr\sin\alpha - n\alpha)\sin(kr\sin\beta - n\beta))$$
$$= \sum_{n=-\infty}^{\infty} \frac{1}{4\pi^4}\int_0^\pi\int_0^\pi\int_0^\pi\int_0^\pi (\cos(kA(\phi,-\theta,-\alpha,-\beta) - nB(\phi,-\theta,-\alpha,-\beta))$$
$$+\cos(kA(\phi,\theta,\alpha,\beta) - nB(\phi,\theta,\alpha,\beta))$$
$$+\cos(kA(\phi,-\theta,\alpha,\beta) - nB(\phi,-\theta,\alpha,\beta))$$
$$+\cos(kA(\phi,\theta,-\alpha,-\beta) - nB(\phi,\theta,-\alpha,-\beta)))\,\mathrm{d}\theta\,\mathrm{d}\phi\,\mathrm{d}\alpha\,\mathrm{d}\beta$$
$$= \sum_{m=-\infty}^{\infty} \frac{1}{2\pi^3}\int_0^\pi\int_0^\pi\int_0^\pi\int_0^\pi (\cos(kA(\phi,\theta,\alpha,\beta))\delta(2\pi m - B(\phi,\theta,\alpha,\beta))$$
$$+\cos(kA(\phi,\theta,-\alpha,-\beta))\delta(2\pi m - B(\phi,\theta,-\alpha,-\beta))$$
$$+\cos(kA(\phi,-\theta,\alpha,\beta))\delta(2\pi m - B(\phi,-\theta,\alpha,\beta))$$
$$+\cos(kA(\phi,-\theta,-\alpha,-\beta))\delta(2\pi m - B(\phi,-\theta,-\alpha,-\beta)))\,\mathrm{d}\theta\,\mathrm{d}\phi\,\mathrm{d}\alpha\,\mathrm{d}\beta \tag{A.1}$$

where we define the functions

$$A(\phi,\theta,\alpha,\beta) = r\sin\phi + r\sin\theta + R\sin\alpha + R\sin\beta \tag{A.2}$$

$$B(\phi,\theta,\alpha,\beta) = \phi + \theta + \alpha + \beta. \tag{A.3}$$

The last line follows from equation (2.16). We can now consider each of these terms separately, starting with the first term

$$\frac{1}{2\pi^3}\int_0^\pi\int_0^\pi\int_0^\pi\int_0^\pi \cos(k(r\sin\theta + r\sin\phi + R\sin\alpha + R\sin\beta))$$
$$\times \sum_{n=-\infty}^{\infty}\delta(2n\pi - (\theta+\phi+\alpha+\beta))\,\mathrm{d}\theta\,\mathrm{d}\phi\,\mathrm{d}\alpha\,\mathrm{d}\beta. \tag{A.4}$$

Given that our variables are restricted to values in the range $[0, \pi]$ the only term in the sum that we need to consider is where $n = 1$. The others are either not within our limits of integration or correspond to single points (i.e. $\theta = \phi = \alpha = \beta = 0$ when $n = 0$) and therefore give zero contribution.

$$\frac{1}{2\pi^3}\int_0^\pi\int_0^\pi\int_0^\pi\int_0^\pi \cos(k(r\sin\theta + r\sin\phi + R\sin\alpha + R\sin\beta))$$
$$\times\,\delta(2\pi - (\theta+\phi+\alpha+\beta))\,\mathrm{d}\theta\,\mathrm{d}\phi\,\mathrm{d}\alpha\,\mathrm{d}\beta$$
$$= \frac{1}{2\pi^3}\int_0^\pi\int_0^\pi\int_0^\pi \cos(k(r\sin\theta + r\sin\phi + R\sin\alpha - R\sin(\theta+\phi+\alpha))\,\mathrm{d}\theta\,\mathrm{d}\phi\,\mathrm{d}\alpha$$
$$= \frac{1}{2\pi^3}\Re\left(\int_0^\pi\int_0^\pi\int_0^\pi \mathrm{e}^{\mathrm{i}k(r\sin\theta + r\sin\phi + R\sin\alpha - R\sin(\theta+\phi+\alpha))}\,\mathrm{d}\theta\,\mathrm{d}\phi\,\mathrm{d}\alpha\right). \tag{A.5}$$

The contribution of this integral to leading order can now be calculated using the method of stationary phase, subject to the condition that the stationary points (denoted by *) satisfy $0 \leqslant 2\pi - \theta^* - \phi^* - \alpha^* \leqslant \pi$ due to integrating over the delta function. The leading order contribution comes from the only stationary point $\theta^* = \phi^* = \alpha^* = \frac{\pi}{2}$ to satisfy the constraint. Therefore as $k \to \infty$,

$$\frac{1}{2\pi^3} \sum_{n=-\infty}^{\infty} \int_0^{\pi}\int_0^{\pi}\int_0^{\pi}\int_0^{\pi} \cos(kr(\sin\theta + \sin\phi) + kR(\sin\alpha + \sin\beta) - n(\theta + \phi + \alpha + \beta))\,\mathrm{d}\theta\,\mathrm{d}\phi\,\mathrm{d}\alpha\,\mathrm{d}\beta \sim \frac{1}{\pi}\sqrt{\frac{1}{\pi k^3 r R(r+R)}} \cos\left(2k(r+R) - \frac{3\pi}{4}\right). \tag{A.6}$$

We follow the same method with the other terms. The second term has the same stationary point as above and so using the method of stationary phase again we find as $k \to \infty$,

$$\frac{1}{2\pi^3} \int_0^{\pi}\int_0^{\pi}\int_0^{\pi}\int_0^{\pi} \cos(kr(\sin\theta + \sin\phi) - kR(\sin\alpha + \sin\beta))) \times \delta(2\pi - (\theta + \phi - \alpha - \beta))\,\mathrm{d}\theta\,\mathrm{d}\phi\,\mathrm{d}\alpha\,\mathrm{d}\beta \sim \frac{1}{\pi}\sqrt{\frac{1}{\pi k^3 r R(r-R)}} \cos\left(2k(r-R) - \frac{\pi}{4}\right). \tag{A.7}$$

Looking at the third and fourth terms we see that these two expressions are equal if we make the substitution $\theta \leftrightarrow \phi$ and use the evenness of cosine, so we can consider just one expression but double its contribution. The remaining two terms give

$$\begin{aligned} &\frac{1}{\pi^3} \sum_{m=-\infty}^{\infty} \int_0^{\pi}\int_0^{\pi}\int_0^{\pi}\int_0^{\pi} \cos(k(r(\sin\theta - \sin\phi) - R(\sin\alpha + \sin\beta))) \\ &\qquad \times \delta(2\pi m - (\theta - \phi - \alpha - \beta))\,\mathrm{d}\theta\,\mathrm{d}\phi\,\mathrm{d}\alpha\,\mathrm{d}\beta \\ &\quad = \frac{1}{\pi^3} \int_0^{\pi}\int_0^{\pi}\int_0^{\pi} \cos(k(r(\sin\theta - \sin\phi) - R(\sin\alpha + \sin(\theta - \phi - \alpha)))\,\mathrm{d}\theta\,\mathrm{d}\phi\,\mathrm{d}\alpha \\ &\quad = \frac{1}{\pi^3} \Re\left(\int_0^{\pi}\int_0^{\pi}\int_0^{\pi} \mathrm{e}^{\mathrm{i}k(r(\sin\theta - \sin\phi) - R(\sin\alpha + \sin(\theta - \phi - \alpha)))}\,\mathrm{d}\theta\,\mathrm{d}\phi\,\mathrm{d}\alpha\right). \end{aligned} \tag{A.8}$$

When we calculate the stationary point of the exponent we find that $\theta^* = \phi^*$ and that when this condition is satisfied we have a stationary point for any value of α. However the condition set by the delta function is that for some integer value m, $0 \leqslant \theta^* - \phi^* - \alpha^* - 2\pi m \leqslant \pi$. Clearly the only value of α in our range of integration for which this is possible is $\alpha = 0$ and therefore we have no contribution from either of these terms. As $k \to \infty$,

$$\sum_{n=-\infty}^{\infty} J_n(kR)^2(J_n(kr)^2 - Y_n(kr)^2) \sim \frac{1}{\pi}\sqrt{\frac{1}{\pi k^3 r R(r+R)}} \cos\left(2k(r+R) - \frac{3\pi}{4}\right) + \frac{1}{\pi}\sqrt{\frac{1}{\pi k^3 r R(r-R)}} \cos\left(2k(r-R) - \frac{\pi}{4}\right). \tag{A.9}$$

We now find the asymptotics of the remaining term in the $\langle u^2 \rangle$ expression. Proceeding as before and using the integral asymptotics already calculated we find that

$$\sum_{n=-\infty}^{\infty} J_n(kr)J_n(kR)Y_n(kr)Y_n(kR) \sim \frac{1}{2\pi}\sqrt{\frac{1}{\pi k^3 r R(r-R)}} \cos\left(2k(r-R) - \frac{\pi}{4}\right) - \frac{1}{2\pi}\sqrt{\frac{1}{\pi k^3 r R(r+R)}} \cos\left(2k(r+R) - \frac{3\pi}{4}\right). \tag{A.10}$$

Combining all of these results gives

$$\langle u^2\rangle \simeq 1 - \sqrt{\frac{R}{\pi kr(r-R)}}\cos\left(2k(r-R) - \frac{\pi}{4}\right). \tag{A.11}$$

Appendix B. Higher order asymptotics

The next order of asymptotics for each of our expressions comes from the second term in the integral expression for $Y_n(x)$ given in equation (2.15) which we have so far ignored. We use Laplace's method to determine the large k asymptotics of this term,

$$\int_0^\infty (\mathrm{e}^{nt} + \mathrm{e}^{-nt}\cos n\pi)\,\mathrm{e}^{-kr\sinh t}\,\mathrm{d}t = \begin{cases} 0 & \text{if } n \text{ is odd,} \\ \frac{2}{kr} & \text{if } n \text{ is even.} \end{cases} \tag{B.1}$$

Obviously, if we have two of these terms multiplying each other then the entire expression would have order k^{-2} so we look at the contribution from one of these terms multiplied by the remaining Bessel functions. For example,

$$\sum_{n=-\infty}^{\infty} J_n(kR)^2 Y_n(kr)^2 \text{ contributes } \frac{2}{kr}\sum_{n=-\infty}^{\infty} J_{2n}(kR)^2 Y_{2n}(kr) \tag{B.2}$$

at this order. For the ease of calculation we can actually consider the sum to be over all orders on the right-hand side because the oddness with respect to order of the Bessel functions results in all odd ordered contributions cancelling. Proceeding as in appendix A we find that integrals do not have any contribution to leading order due to the absence of a stationary point. Following this method for the $\langle u_r^2\rangle$ expression gives zero immediately because differentiating the integrand in equation (B.1) with respect to r gives an extra factor of $-\sinh t$ which equals zero at the point we expand around. This suggests that our next order term will be of order $k^{-\frac{3}{2}}$ and can be found by looking again at the stationary phase asymptotics. From [15]

$$\begin{aligned}\int_{\mathcal{D}} g(\mathbf{x})\exp(\mathrm{i}\lambda\phi(\mathbf{x}))\,\mathrm{d}\mathbf{x} \sim \left(\frac{2\pi}{\lambda}\right)^{\frac{n}{2}} \exp\left(\frac{\pi\mathrm{i}}{4}\mathrm{sig}\big(\phi_{x_i}\phi_{x_j}\big) + \mathrm{i}\lambda\phi(\mathbf{x}_0)\right) \\ \times\left(\frac{g(\mathbf{x}_0)}{\sqrt{\left|\det\big(\phi_{x_i}\phi_{x_j}\big)\right|}} + \frac{\mathrm{i}}{2}\lambda^{-1}\Delta\mathrm{G}_0\right),\end{aligned} \tag{B.3}$$

where n is the dimension of $\mathbf{x}$, $\mathbf{x}_0$ is the stationary point of $\phi(\mathbf{x})$ and sig$M$ is the number of positive eigenvalues of M minus the number of negative eigenvalues. The first term on the right-hand side is stated for each of our expressions in equations (2.17)–(2.19), the second term is given by,

$$\begin{aligned}\Delta\mathrm{G}_0 = \left(\left|\det\big(\phi_{x_i}\phi_{x_j}\big)\right|\right)^{-\frac{1}{2}}\big[-\phi_{x_s x_r x_q} A_{sq} A_{rp}(g_0)_{x_p} + \mathrm{Tr}(CA) \\ + g_0\big(\phi_{x_p x_q x_r}\phi_{x_s x_t x_u}\big(\tfrac{1}{4}A_{ps}A_{qr}A_{tu} + \tfrac{1}{6}A_{ps}A_{qt}A_{ru}\big) - \tfrac{1}{4}\phi_{x_p x_q x_r x_s}A_{pr}A_{qs}\big)\big]_{x=x_0}.\end{aligned} \tag{B.4}$$

Here the summation convention is observed with repeated indices summed from 1 to n. A and C are defined by

$$A_{pq}\phi_{x_q x_r} = \delta_{pr} \qquad C = \big((g_0)_{x_p x_q}\big). \tag{B.5}$$

Using these formulae our final asymptotics as $k \to \infty$ are

$$\langle u^2\rangle \sim 1 \mp \sqrt{\frac{R}{\pi kr(r-R)}}\left(\cos\left(2k(r-R) - \frac{\pi}{4}\right) - \frac{r^2 - 7rR + R^2}{16krR(r-R)}\sin\left(2k(r-R) - \frac{\pi}{4}\right)\right) \tag{B.6}$$

$$\left\langle u_r^2 \right\rangle \sim \frac{k^2}{2}\left(1 \pm 2\sqrt{\frac{R}{\pi kr(r-R)}}\left(\cos\left(2k(r-R)-\frac{\pi}{4}\right)\right.\right.$$
$$\left.\left. - \frac{r^2+9rR-7R^2}{16krR(r-R)}\sin\left(2k(r-R)-\frac{\pi}{4}\right)\right)\right). \tag{B.7}$$

It is worth noting that these expressions are not as accurate as those calculated in section 2.1 for small values of k because in this regime the functions are dominated by the higher order terms which are of the order $k^{-\frac{3}{2}}$, since $(r-R)$ is small.

References

[1] Berry M V 1977 Regular and irregular semiclassical wavefunctions *J. Phys. A: Math. Gen.* **10** 2083–91
[2] Blum G *et al* 2002 Nodal domain statistics: a criterion for quantum chaos *Phys. Rev. Lett.* **88** 114101
[3] Berry M V and Dennis M R 2000 Phase singularities in isotropic random waves *Proc. R. Soc. Lond.* A **456** 2059–79
[4] Foltin G 2003 Counting nodal domains *Preprint* nlin.CD/0302049 v1
[5] Berry M V and Dennis M R 2001 Knotted and linked phase singularities in monochromatic waves *Proc. R. Soc. Lond.* A **457** 2251–63
[6] Bogomolny E and Schmit C 2002 Percolation model for nodal domains of chaotic wave functions *Phys. Rev. Lett.* **88** 114102
[7] Bies W E and Heller E J 2002 Nodal structure of chaotic eigenfunctions *J. Phys. A: Math. Gen.* **35** 5673–85
[8] Berry M V 2002 Statistics of nodal lines and points in chaotic quantum billiards: perimeter corrections, fluctuations, curvature *J. Phys. A: Math. Gen.* **35** 3025–38
[9] Berry M V and Ishio H 2002 Nodal densities of gaussian random waves satisfying mixed boundary conditions *J. Phys. A: Math. Gen.* **35** 5961–72
[10] Bies W E *et al* 2003 Quantum billiards and constrained random wave correlations *J. Phys. A: Math. Gen.* **36** 1605–13
[11] Urbina J D and Richter K 2003 Supporting random wave models: a quantum mechanical approach *J. Phys. A: Math. Gen.* **36** L495–L502
[12] Urbina J D and Richter K 2004 Semiclassical construction of random wave functions for confined systems *Phys. Rev.* E **70** 015201(R)
[13] Urbina J D 2004 private correspondence
[14] Abramowitz M and Stegun I A 1970 *Handbook of Mathematical Functions* (New York: Dover)
[15] Bleistein N and Handelsman R A 1986 *Asymptotic Expansions of Integrals* (New York: Dover)
[16] Dennis M R 2001 Topological singularities in wave fields *PhD Thesis* University of Bristol
[17] Watson G N 1944 *A Treatise on the Theory of Bessel Functions* 2nd edn (London: Cambridge University Press)
[18] Gradshteyn I S and Ryzhik I M 1965 *Table of Integrals, Series, and Products* (New York: Academic)